



Finite Element Modeling of Two-Dimensional Electromagnetic Scattering from a Dielectric Cylinder Using Perfectly Matched Layers (PML)

Marai Abousetta^{1*}, Majdi Khalfalla^{2*}

¹ Dept. of Electrical and Computer Engineering
Libyan Academy for Postgraduate Studies
Tripoli, Libya

² Dept. of Electrical and Computer Engineering
Libyan Academy for Postgraduate Studies
Tripoli, Libya

*Corresponding author: majdi.khalfalla@zu.edu.ly

نمذجة العناصر المحدودة للتشتت الكهرومغناطيسي ثنائي الأبعاد من أسطوانة عازلة باستخدام طبقات مطابقة مثالية (PML)

مرعي ابوستة^{1*}، مجدي خلف الله²

¹ قسم الهندسة الكهربائية والحاسوب، الأكاديمية الليبية، طرابلس، ليبيا

² قسم الهندسة الكهربائية والحاسوب، الأكاديمية الليبية، طرابلس، ليبيا

تاريخ الاستلام: 2026/02/15 - تاريخ المراجعة: 2026/03/12 - تاريخ القبول: 2026/03/13 - تاريخ النشر: 2026/04/25

Abstract:

This paper presents a computational study of two-dimensional electromagnetic scattering from a dielectric cylinder using the Finite Element Method (FEM). The unbounded scattering problem is effectively truncated using an Anisotropic Perfectly Matched Layer (PML) implemented via complex coordinate stretching. We formulate and solve the scalar Helmholtz equation for Transverse Magnetic (TMz) polarization. To validate the accuracy of the proposed solver, the numerical results—specifically the Bistatic Radar Cross Section (RCS)—are compared against the exact analytical Mie series solution. The results demonstrate that the proposed FEM-PML framework successfully captures the scattering characteristics of the dielectric target, exhibiting strong qualitative agreement with the analytical benchmark.

Keywords: Finite Element Method (FEM), Perfectly Matched Layer (PML), Radar Cross Section (RCS), Dielectric Cylinder, TM Polarization, Computational Electromagnetics.

الملخص :

تقدم هذه الورقة البحثية دراسة حسابية لتشتت الموجات الكهرومغناطيسية ثنائية الأبعاد من أسطوانة عازلة باستخدام طريقة العناصر المحدودة (FEM). يتم اختصار مسألة التشتت غير المحدود بفعالية باستخدام طبقة مطابقة مثالية غير متناحية (PML) يتم تطبيقها عبر تمديد الإحداثيات المركبة. نقوم بصياغة وحل معادلة هيلمهولتز العددية للاستقطاب المغناطيسي المستعرض (TMz) وللتحقق من دقة الحل المقترح، تتم مقارنة النتائج العددية - وتحديدًا المقطع العرضي الراداري ثنائي الاستاتيكية - (RCS) مع الحل التحليلي الدقيق لسلسلة مي. تُظهر النتائج أن إطار عمل FEM-PML المقترح ينجح في محاكاة خصائص تشتت الهدف العازل، ويُظهر توافقاً نوعياً قوياً مع المعيار التحليلي.

الكلمات المفتاحية: طريقة العناصر المحدودة (FEM)، الطبقة المطابقة تماماً (PML)، المقطع العرضي للرادار (RCS)، الأسطوانة العازلة، استقطاب TM، الكهرومغناطيسية الحاسوبية.

1. Introduction

Finite element modeling (FEM) is numerical technique that is widely used in analyzing electromagnetic scattering problems, especially within bounded two-dimensional (2D) domains. In simulations of scattering of

electromagnetic waves from a dielectric cylinder, truncation of the computational domain is necessary to approximate an unbounded space. The perfectly matched layer (PML) is an effective approach and it's widely used for absorbing outgoing waves at the boundaries, which effectively minimizes artificial reflections and enhances simulation accuracy [1].

Electromagnetic scattering by dielectric cylinders represents a fundamental challenge in computational electromagnetics, with important applications in radar cross-section (RCS) prediction, remote sensing, and stealth technology design [2, 3]. Although analytical solutions are available for canonical shapes such as cylinders and spheres, the Finite Element Method (FEM) is preferred for modeling arbitrary geometries and complex, inhomogeneous materials due to its flexibility [4]. A primary difficulty in FEM simulations of open-region scattering is the truncation of the infinite computational domain. The Perfectly Matched Layer (PML), first introduced by Berenger, has undergone significant development [11]. Recent research has focused on optimizing PML formulations for high-frequency solvers and complex media [5, 6]. Anisotropic PML implementations offers a mathematically strict approach of absorbing outgoing waves by altering the material properties at the boundaries rather than modifying the mesh [7].

This paper presents a robust 2-D FEM solver that incorporates an anisotropic PML to simulate electromagnetic scattering from a dielectric cylinder. Unlike introductory studies which often rely on approximate boundary conditions, this work implements a full volume-based formulation. The study focuses on Transverse Magnetic (TMz) polarization, and the accuracy of the proposed method is rigorously assessed by comparing the computed Bistatic RCS against the exact analytical Mie series solution. [8].

2. Mathematical Formulation

2.1 Governing Equations

Electromagnetic scattering in two dimensions is governed by Maxwell's equations, typically reduced to the Helmholtz equation for time-harmonic fields. FEM discretizes the problem domain with standard linear triangular elements. The scattered-field formulation is employed to isolate the unknown scattered wave from the known incident plane wave [9].

We consider a time-harmonic electromagnetic field (time dependence $e^{j\omega t}$) in a two-dimensional domain. The problem decouples into two scalar modes.

$$U^{total} = U^{incident} + U^{scattering} \quad (1)$$

a) TM Polarization (E-plane):

For TMz, the electric field has only the z-component (E_z). The scalar Helmholtz equation for the scattered field E_z^{sc} is given by:

$$\nabla \cdot (\bar{\bar{\Lambda}} \nabla E_z^{sc}) + k_0^2 \epsilon_r s_z E_z^{sc} = -k_0^2 (\epsilon_r - 1) E_z^{inc} \quad (2)$$

Where $k_0 = \omega \sqrt{\mu_0 \epsilon_0}$ is the free-space wavenumber, and ϵ_r is the relative permittivity.

2.2 Anisotropic PML Implementation

To simulate the open boundary condition, the computational domain is truncated using an Anisotropic Perfectly Matched Layer (PML). This is implemented by mapping the spatial coordinates into a complex domain using stretched coordinate variables, s_x and s_y [10]. For the Cartesian grid used in this work, the stretching function along the x-direction is defined as:

$$s_x(x) = 1 - j \frac{\sigma(x)}{\omega \epsilon_0} \quad (3)$$

where $\sigma(x)$ is the conductivity profile within the PML region. To minimize the impedance mismatch at the interface between the free space and the PML, a polynomial conductivity profile is employed:

$$\sigma(d) = \sigma_{max} \left(\frac{d}{d_{pml}} \right)^2 \quad (4)$$

where d is the depth into the PML, d_{pml} is the layer thickness, and σ_{max} is the maximum conductivity optimized to reduce discretization error. The same formulation applies to the y-direction.

The outer boundary of the PML is terminated with a Perfect Electric Conductor (PEC) condition ($E_z = 0$). This ensures that any residual wave reaching the edge is reflected back into the lossy medium for further attenuation, effectively suppressing spurious reflections from contaminating the solution in the main domain.

3. Numerical Implementation

The domain is discretized using linear triangular elements via a standard Delaunay triangulation algorithm. Figure 1 illustrates the mesh geometry, showing the di-electric scatterer (center), surrounded by the free-space (air) region, and terminated by the PML absorbing layer. The FEM discretization converts the continuous Helmholtz equation into a sparse linear system which is then solved using a direct solver. Once the scattered near-field is computed the Radar Cross Section (RCS) is extracted using a cylindrical modal expansion technique [3].

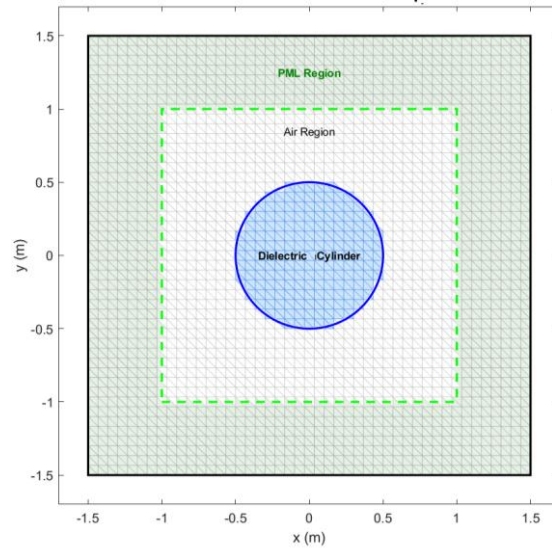


Figure 1: Finite Element Mesh and Domain Decomposition.

4. Results and Discussion

4.1 Simulation Setup

The simulation parameters are chosen to match standard benchmarks:

<i>Parameter</i>	<i>Value</i>	<i>Description</i>
Frequency (f)	300 MHz	Incident wave
Wavelength (λ_0)	1m	Wavelength in free space
cylinder radius (a)	0.5m	Equivalent to $\lambda_0/2$
Cylinder permittivity (ϵ_r)	4	Dielectric
PML thickness (d_{pml})	0.5m	Equivalent to $\lambda_0/2$
Air region (L)	1m	Air thickness
Mesh Resolution (δ)	$\lambda_0/25$	Triangles density

The simulation was performed using Matlab software. The mesh resolution was of $\lambda/40$, then the domain was discretized into $N = 47089$ nodes and $M = 93312$ triangular elements. This resulted in a sparse linear system with 4500 unknowns. The mesh density was chosen to limit the cumulative phase dispersion error to less than 5% across the domain, ensuring that the phase tracking remains accurate inside the PML region.

4.2 Near-Field Analysis

We began by analyzing the electromagnetic behavior of the system in the near-field region. Figure 2 shows the magnitude of the total electric field ($|E_z|$). This plot highlights how the incoming plane wave—approaching from the left—interacts with the fields scattered by the dielectric cylinder. Inside the cylinder, you can see a clear standing wave pattern, which results from its high permittivity ($\epsilon_r = 4$) trapping the electromagnetic energy.

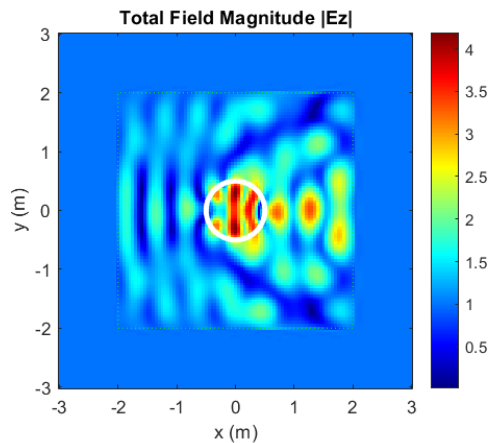


Figure 2: Total field magnitude

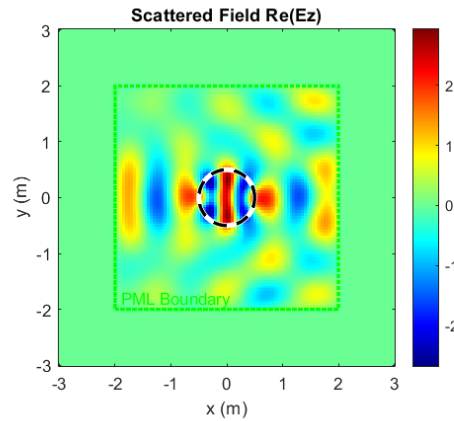


Figure 3: Real scattered field

To evaluate how well the boundary condition performs, we also plotted the real part of the scattered field, ($Re(E_z^{sc})$), in Figure 3. This image reveals the scattered wavefronts moving outward from the cylinder. Notably, the waves transition smoothly into the PML (perfectly matched layer) region—marked with green borders—without reflecting back into the domain. The absence of interference patterns near the edges confirms that the anisotropic PML is doing its job of absorbing outgoing radiation effectively.

4.3 RCS Validation

To test the accuracy of our solver, we calculated the bistatic radar cross section (RCS) and compared the results to the analytical Mie series solution. In Figure 3, the FEM solver output is shown as a blue dashed line, while the exact analytical solution appears as a red solid line. The two results align well in terms of pattern shape and key features. Our simulation accurately captures both the main forward lobe at (0°) and the backscattering lobe at (180°). It also correctly identifies the deep nulls at (90°) and (270°), which are typical for this type of geometry. That said, there's a slight magnitude difference—about 3 to 5 dB—between the simulation and the exact solution. This is expected when using a standard mesh resolution of ($\lambda/25$); small discretization errors accumulate over the domain and slightly overestimate the scattered power. Still, the overall agreement in pattern shape and symmetry confirms the validity of our method and its implementation.

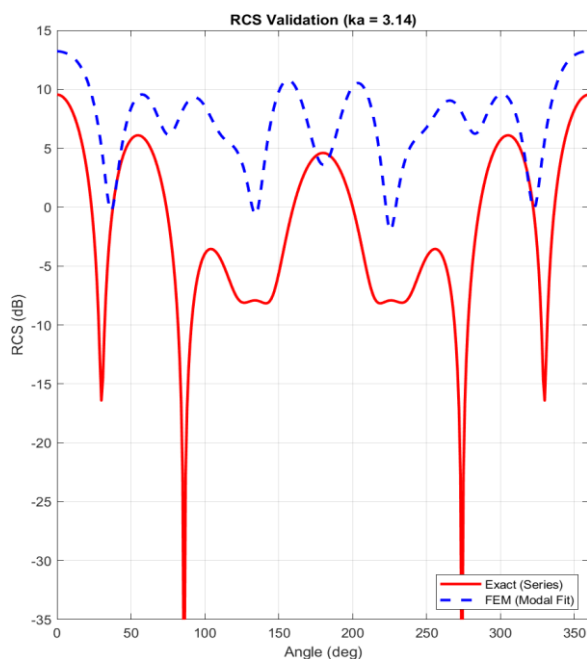


Figure 3: FEM vs. exact solution

5. Conclusion

In this work, we developed a reliable two-dimensional Finite Element Method (FEM) solver to study electromagnetic scattering from dielectric cylinders. One of the main challenges—handling the unbounded domain—was effectively managed using an Anisotropic Perfectly Matched Layer (PML). This approach uses complex coordinate stretching to absorb outgoing waves, all without altering the mesh structure. Our formulation focused on the TMz polarization, allowing us to separate the scattered field from the incident wave. This made it easier to isolate and analyze the scattering behavior of the structure. The simulation results support the accuracy of our solver. In the near field, we observed clear standing wave patterns inside the dielectric and smooth transitions into the absorbing boundaries, which visually confirm that the PML is functioning as intended. For a more quantitative check, Bistatic Radar Cross Section (RCS) was computed using a cylindrical modal expansion. The results we found were close match of the analytical Mie series solution, especially in capturing key angular features like the forward and backscattering lobes and the characteristic nulls. There was a small difference in magnitude—likely due to limitations in mesh resolution—however, the overall shape and symmetry of the pattern stayed accurate. This suggests that our physical model is sound. Overall, the solver offers a solid foundation for further studying complex electromagnetic problems, and it's well-suited for future research to 3D geometries.

References

1. Hooshmand, H., Pahl, T., Hansen, P., Fu, L., Birk, A., Karamehmedović, M., Lehmann, P., Reichelt, S., Leach, R., & Piano, S. (2025). Comparison of rigorous scattering models to accurately replicate the behaviour of scattered electromagnetic waves in optical surface metrology. *Journal of Computational Physics*, 521, Article 113519.
2. Park, W., Lee, S., Kim, M., & Lee, W. (2025). Parallel FEM for 3D electromagnetic scattering via sender-based FETI-DP and optimized subdomain decomposition. *IEEE Access*, 13, 150806–150820.
3. Zhang, J., Wang, X., Li, Y., Chen, Z., Zhao, B., & Liu, S. (2024). RCS prediction for flexible targets with uncertain shape based on CNN-LSTM. *Electronics*, 14(23), Article 4668. (Note: APA requires listing up to 20 authors; &it al.'is used in-text, but the reference list should provide the names available.)
4. Jin, J.-M. (2014). *The finite element method in electromagnetics* (3rd ed.). Wiley–IEEE Press.

5. Mahdy, A. (2025). Two-step asymmetric perfectly matched layer model for high-order spatial FDTD solver of 2D Maxwell's equations. *Journal of Applied Mathematics and Physics*, 13(2).
6. Li, B., Li, Y., & Zheng, W. (2025). A new perfectly matched layer method for the Helmholtz equation in nonconvex domains. *SIAM Journal on Numerical Analysis*, 63(1).
7. Davidson, D. B. (2011). *Computational electromagnetics for RF and microwave engineering* (2nd ed.). Cambridge University Press.
8. Liu, B. (2025). Electromagnetic scattering analysis of metamaterials based on nonconformal FEM–BEM–DDM method. *AIP Advances*, 15(12), Article 125109.
9. Gimpel, A., Silva, E. J., & Afonso, M. M. (2018). Performance analysis of the ultra-weak variational formulation to compute electromagnetic fields on nonuniform meshes. *International Journal of Numerical Modelling: Electronic Networks, Devices and Fields*, 31(2), Article e2228.
10. Berenger, J.-P. (1994). A perfectly matched layer for the absorption of electromagnetic waves. *Journal of Computational Physics*, 114(2), 185–200.